

XV. PHYSICAL ELECTRONICS AND SURFACE PHYSICS*

Academic and Research Staff

Prof. R. E. Stickney
Dr. M. L. Shaw

Graduate Students

F. W. Eberle
D. L. Fehrs

J. W. Gadzuk
W. Greaves
H. C. Juvkam-Wold

D. S. Shupe
S. Yamamoto

RESEARCH OBJECTIVES

The general purpose of our research program is to investigate the interaction of electrons, ions, atoms, molecules, and electromagnetic radiation with solid surfaces. At present, we are concentrating on the following problems.

1. Adsorption of Gases and Vapors on Solid Surfaces

The work function of a thermionic cathode may be altered by allowing certain gases or vapors to adsorb upon the surface. Our theoretical and experimental studies are concerned primarily with the adsorption of oxygen and/or cesium on single-crystal refractory metal surfaces. We are attempting to relate the change in work function and desorption energy to the coverage, crystallographic structure, and bare work function of the substrate.

2. Catalysis and Oxidation

Using mass spectrometric techniques, we are investigating the catalytic formation of ammonia on iron and the oxidation of tungsten. Our principal objective is to determine the dependence of these reactions on temperature, pressure, and material properties.

3. Scattering of Gas Atoms and Molecules from Solid Surfaces

Recently, we have developed a simple classical theory for the collisions of atoms and molecules with solid surfaces. The results predict the scattering pattern and energy and momentum transfer. A quantum-mechanical model has also been investigated. In addition to continuing these theoretical approaches, we now are developing an experimental apparatus for measuring the scattering patterns.

4. Photoinduced Surface Processes

Measurements of the photoelectric emission from solids provides us with an additional means of studying surfaces. We plan to determine the photoelectric properties of single-crystal surfaces that are partially covered with adsorbed atoms. Along this same line, we shall look for the existence of photoinduced ion emission from cesiated surfaces.

R. E. Stickney

*This work was supported by the National Aeronautics and Space Administration (Grant NGR-22-009-091), the M. I. T. Cabot Solar Energy Fund, and the Joint Services Electronics Programs (U. S. Army, U. S. Navy, and U. S. Air Force) under Contract DA 36-039-AMC-03200(E).

(XV. PHYSICAL ELECTRONICS AND SURFACE PHYSICS)

A. CONTACT POTENTIAL MEASUREMENTS OF THE ADSORPTION OF O₂ ON (110) Ta

1. Introduction

During the past two years, we have developed an experimental apparatus for measuring the change in contact potential resulting from the adsorption of various chemical elements on metallic surfaces.¹ We shall report results recently obtained for the adsorption of O₂ on (110) Ta. These results are particularly interesting because they are contrary to the majority of previous experimental results and existing theoretical predictions.

2. Apparatus

Since the apparatus has been described in detail elsewhere,¹ only the major features will be mentioned here. To avoid contamination by background gases the apparatus was mounted within a large Varian ultrahigh vacuum system. With a combination of ion pumping, liquid-nitrogen cryopumping, and titanium sublimation pumping, the background pressure during these runs could be maintained in the mid 10⁻¹¹ Torr range ($\sim 4-5 \times 10^{-11}$ Torr).

The specimen studied was a tantalum ribbon, 0.0025 × 0.127 × 3.0 cm, mounted upon a rotatable shaft. The ribbon was cut from a larger specimen which, when received, was reported to have a surface oriented in the (110) direction. Unfortunately, the exact orientation of the specimen used in the present study has not yet been determined by x-ray diffraction. The surface was cleaned by direct resistive heating to $\sim 2500^\circ\text{K}$, with occasional flashes to $\sim 2750^\circ\text{K}$.

Changes of substrate work function, because of oxygen adsorption, have been measured by the contact-potential method. For this measurement the target was positioned before a simple electron gun. To insure the constant-emitter conditions required by the contact-potential method, the gun filament was continually run at $\sim 2100^\circ\text{K}$. As well as measuring changes in the surface work function, it was possible to measure the thermionic work function of the bare surface at a thermionic measurement station.

A diffusion leak was used to flood the system to the desired oxygen pressure. The maximum static pressure that could be obtained in the presence of all available pumping was $\sim 10^{-7}$ Torr.

A series of auxiliary runs utilized a General Electric Company monopole partial pressure analyzer. This made it possible to determine the composition of the background gas and, more important, to check the purity of the oxygen admitted by the diffusion leak.

3. Experimental Method and Procedure

The theory, advantages, and limitations of the contact-potential method have been adequately discussed elsewhere¹⁻³ and will only be briefly mentioned here. Basically we have two electrodes, the electron gun filament and the (110) tantalum target, which form a diode. If we maintain constant conditions at the emitter (electron gun filament), then any changes in the current-voltage characteristic of the diode are due to changes in the properties of the collector (110 Tantalum). In particular, the simple theory of a thermionic diode shows that a voltage shift of the Boltzmann portion of the current-voltage plot will be equal to the change of the collector work function if the reflection coefficient remains constant. The reference point, from which changes are measured, is the current-voltage plot taken when both electrodes are clean.

In this study the experimental method was implemented by the following procedure. After a clean current-voltage plot had been obtained, the diffusion leak was turned on and the system allowed to reach a steady O₂ pressure. Once this steady pressure had been reached, the target was flash-cleaned and current-voltage plots were made as a function of time.

Since these plots could only be taken at 300°K, it was desirable to consider also the effect of target temperature upon the adsorption process. Unfortunately, it was not possible to make the work function-time measurements at elevated temperatures. Instead, we could only study the effect of temperature during the time of adsorption. A few runs were made in which the surface was exposed to the same total oxygen flux, but with the surface maintained at different temperatures (always higher than 300°K) during the time of adsorption. After the adsorption interval, the system was pumped back to the 10⁻¹¹ Torr range and the surface cooled to 300°K. The current-voltage plots were then taken at room temperature.

In addition to oxygen adsorption runs, a few oxygen desorption runs were made. In these a certain oxygen coverage was established, and then the system was pumped back to the 10⁻¹¹ Torr range. The surface was then flashed to some temperature for 15 sec and, upon cooling to 300°K, a current-voltage plot was taken. The 15-sec flashes were continued by stepping the temperature to a higher value each time until the clean surface plot was finally obtained. These runs enabled us to check the reversibility of the data and to estimate the desorption energy of oxygen on (110) Ta.

4. Experimental Results

a. Thermionic Work Function

Measurements of thermionic emission from the target were used to calculate the effective work function.³ A value of $\phi_o = 4.73 \pm 0.01$ eV was obtained for 5 measurements in the temperature range ~1570°K to ~2360°K.

(XV. PHYSICAL ELECTRONICS AND SURFACE PHYSICS)

b. Mass Spectrometer Measurements

When the total pressure was in the mid 10^{-11} Torr range, mass spectrometer analysis of the background gas showed the major components to be H_2O (~18%), He (~16%), CO (~13%), O (~13%), and CO_2 (~10%). Present in smaller amounts were OH, H, Ne, O_2 , and H_2 . We believe that O, H, and OH are produced in the spectrometer as a result of dissociation and/or desorption induced by electron bombardment.

The oxygen diffusion leak was analyzed at two different steady-state oxygen pressures. At an oxygen pressure of $\sim 10^{-9}$ Torr, none of the background contaminant peaks, such as CO and CO_2 , showed any perceptible increase over the initial background values. The temperature of the diffusion leak was increased until a steady-state pressure of $\sim 10^{-7}$ Torr was established. At this pressure the only significant components were O_2 , O, and CO. The combination of O and O_2 formed approximately 97% of the total pressure, and CO formed approximately 3%. These results indicate, particularly at lower oxygen pressures, that contamination from such components as CO should not be a major problem.

c. Oxygen Adsorption on (110) Ta

In Fig. XV-1, a portion of the results for oxygen adsorption are shown in the form of work-function change as a function of oxygen exposure. The oxygen exposure is

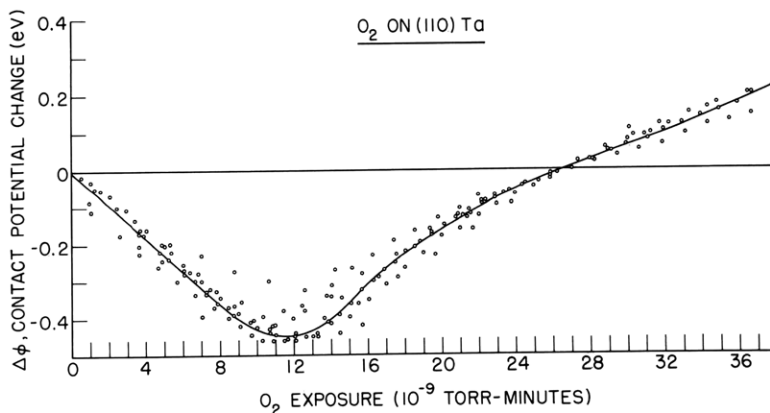


Fig. XV-1. Experimental data for oxygen adsorption on (110) Ta at 300°K; low exposure region.

defined simply as the product of oxygen pressure times the time. In terms of the actual integrated particle flux, an exposure of 1×10^{-9} Torr-minutes, for example, is equal to 4.27×10^{13} oxygen atoms/cm².

(XV. PHYSICAL ELECTRONICS AND SURFACE PHYSICS)

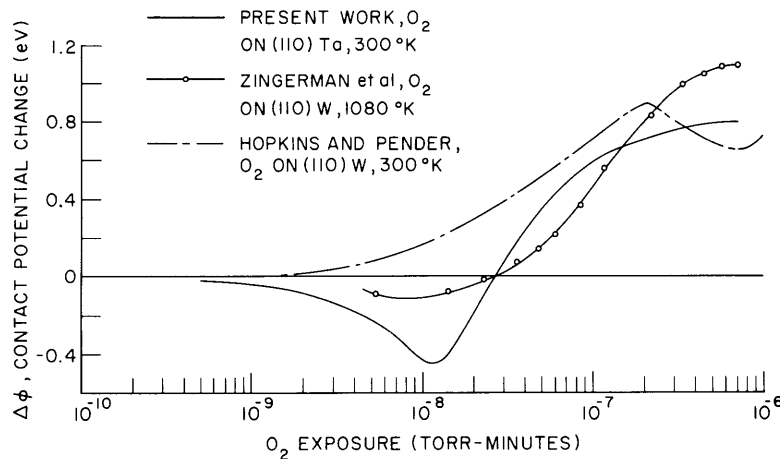


Fig. XV-2. Experimental data for oxygen adsorption on (110) Ta at 300°K compared with data for oxygen on (110) tungsten.

For clarity, only the extreme values of the data and the average curve are shown in Fig. XV-1. The actual plot contains approximately 200 points from 8 separate runs. Also, Fig. XV-2 does not represent the raw data, for there has been some attempt to correlate the raw data and reduce initial scatter that occurred primarily because of inaccuracies of pressure measurement. The correlation has been achieved by multiplying the curve for each run by a factor that would make the curve pass through $\Delta\phi = 0$ at an exposure of $\sim 27 \times 10^{-9}$ Torr-minutes. In the raw data the exposure at which $\Delta\phi$ went to zero ranged from 23 to 30×10^{-9} Torr-minutes, and the average value was $\sim 27 \times 10^{-9}$ Torr-minutes. As we shall see, an interesting comparison can be made between this arbitrary correlation point and other recently published data.

The most interesting feature of the data is that below exposures of 27×10^{-9} Torr-minutes, oxygen adsorption produces a decrease in the work function of the surface. The curve shows a minimum at an exposure of $\sim 12 \times 10^{-9}$ Torr-minutes where the work function has decreased by ~ 0.45 eV. Though most of the runs in Fig. XV-2 were made at oxygen pressures in the low 10^{-9} Torr range, two runs were made in the middle to high 10^{-8} Torr range, and the points fell within the extremes shown in Fig. XV-2. To insure that the decrease in work function was not due to oxygen adsorption upon the electron-gun filament, this filament was usually flashed to $\sim 2500^\circ$ K during the course of a run. No effect was ever seen, thereby indicating that the filament remained uncontaminated. Beyond an exposure of $\sim 40 \times 10^{-9}$ Torr-minutes there are data from only 3 runs. These data are fairly consistent, however, and their average is included in Fig. XV-2, which covers the entire exposure range. Beyond $\sim 27 \times 10^{-9}$ Torr-minutes the work function increases, at first rapidly and then more slowly, tending toward a plateau where the work function has increased by ~ 0.8 eV.

(XV. PHYSICAL ELECTRONICS AND SURFACE PHYSICS)

d. Oxygen Desorption from (110) Ta

The results of one desorption run are shown in Fig. XV-3 where the change in work function (always related to the clean surface) is plotted as a function of the temperature of the consecutive 15-sec flashes. Although the quantitative reproducibility of the desorption runs was rather poor in the plateau region of the curve, the qualitative

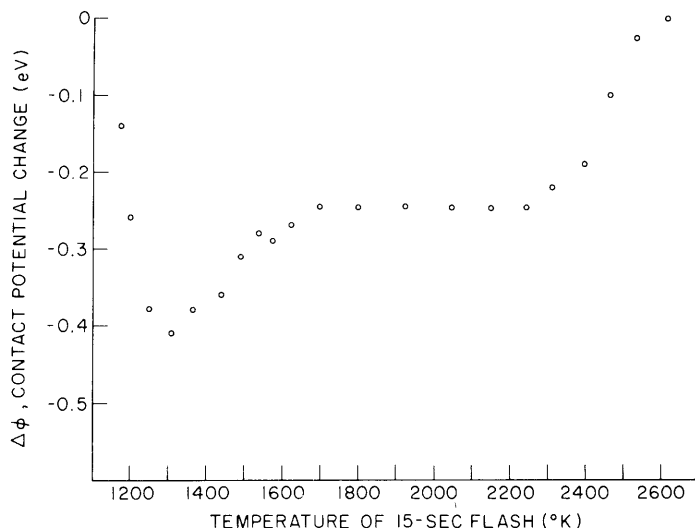


Fig. XV-3. Experimental data for oxygen desorption from (110) Ta.

features were consistently reproduced. In particular, the flashing procedure always reproduced the negative $\Delta\phi$ region of the curve. Also, the negative $\Delta\phi$ always remained up to $\sim 2600^{\circ}$ K, where the clean surface was restored. This, then, may indicate a reversibility for the adsorption process. Also, the high-temperature portion has been used to estimate the desorption energy for oxygen on (110) Ta. An assumption of first-order kinetics (i. e., that the oxygen desorbs as atoms⁴) gives a desorption energy of ~ 6 eV or ~ 138 kcal/mole.

e. Elevated-Temperature Runs

Whereas the desorption data were obtained in an attempt to determine the effect of temperature on an existing adsorbed film, the data shown in Fig. XV-4 resulted from attempts to investigate the effect of elevated temperature on the adsorption process. Runs were made at $\sim 1000^{\circ}$, 1175° , and 1430° K. At each temperature, the surface was subjected to an oxygen exposure of $\sim 11 \times 10^{-9}$ Torr-minutes. After exposure, and upon cooling to 300° K, the resulting work-function change was measured. In Fig. XV-4 the results show the work-function change as a function of surface temperature during adsorption.

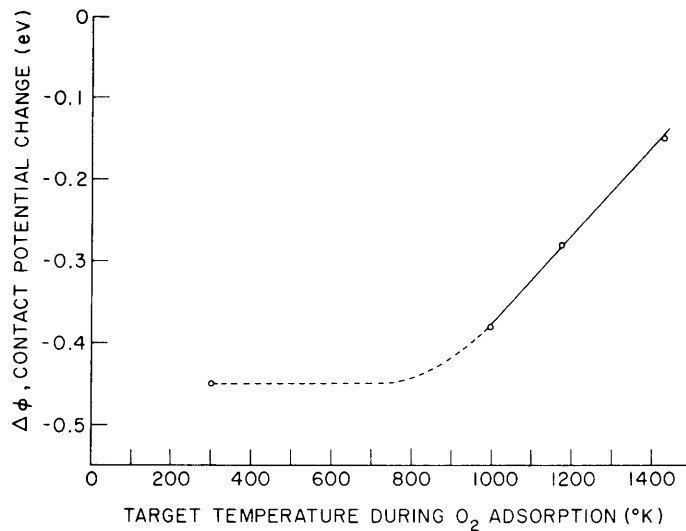


Fig. XV-4. Contact potential change at 300°K as a function of surface temperature during adsorption.

Although the data are insufficient to allow us to draw definite conclusions, two points may be noted. First, for an exposure of 11×10^{-9} Torr-minutes, the work function is observed to decrease for all temperatures in the range 300°-1430°K. Second, the absolute value of the change decreases with increasing temperature. With regard to the first point, it was expected initially that the occurrence of the work-function reduction was due to a metastable state which might disappear at higher temperatures. The results shown in Figs. XV-3 and XV-4 indicate that this expectation may be incorrect. Concerning the second point, there are several possible explanations, and only the simplest will be mentioned here. As may be seen in Fig. XV-1, an exposure of 11×10^{-9} Torr-minutes is near the minimum of the curve at 300°K. If fewer particles remain on the surface at higher temperatures, we would expect from Fig. XV-1 that the absolute value of $\Delta\phi$ would decrease. There are two major possibilities for less oxygen remaining at higher temperatures. First, the sticking probability⁵ for oxygen upon tantalum may decrease with temperature; and second, significant desorption and/or migration of oxygen may occur at higher temperatures. Judging from the desorption data of Fig. XV-3, and owing to the lack of any theoretical or experimental data to support the plausibility of the first hypothesis, the desorption and/or migration hypothesis seems to be more reasonable.

f. Comparison with Existing Data

In Fig. XV-2, the data are compared with two recent sets of data for oxygen adsorption upon (110) tungsten. The data of Hopkins and Pender,⁶ obtained at 300°K by the Kelvin technique, show a work-function change that is always positive. On the other

(XV. PHYSICAL ELECTRONICS AND SURFACE PHYSICS)

hand, the data of Zingerman and co-workers,⁷ obtained at 1080°K by the same technique used in our work, are qualitatively similar to our data. Initially, there is a slight decrease in the work function, followed later by an increase. Since Zingerman et al. did not know the intensity of their oxygen beam, it was not possible to assign a quantitative exposure scale. For qualitative comparison only, a scale was assigned by making their data pass through zero at an exposure of 27×10^{-9} Torr-minutes.

Germer and May⁸ have recently published data from a low-energy electron-diffraction (LEED) study of oxygen adsorption upon (110) tungsten. Several interesting inferences may be drawn from their data:

1. It appeared that, even at 300°K, oxygen adsorption occurred by reconstruction such that the oxygen occupied substitutional sites in the surface lattice.
2. Average oxygen sticking probabilities at 300°K were inferred for the ranges 0-1/2 monolayer, 1/2-3/4 monolayer, and 3/4-1 monolayer of oxygen. (A monolayer is defined as 1.425×10^{15} atoms/cm².) For 0-1/2 monolayer the average value was ~ 0.6 ; for 1/2-3/4 monolayer it fell sharply to ~ 0.003 ; and for 3/4-1 monolayer it fell to less than 0.003.
3. The half-monolayer structure occurred at an oxygen exposure of $\sim 27 \times 10^{-9}$ Torr-minutes. As shown in Figs. XV-1 and XV-2, our present data for oxygen on (110) Ta indicate that $\Delta\phi$ passes through zero at this value of exposure. At present, it is not clear whether this point is mere coincidence or a matter of physical significance.

g. Comparison of Results with Theoretical Predictions

The data are unusual, in that oxygen adsorption on the (110) Ta initially produces a decrease in the work function. With the use of the concept of electronegativity,⁹ oxygen adsorption should lead to a dipole moment that is directly proportional to $X_{\text{Ta}} - X_{\text{O}}$, the difference in the electronegativities of tantalum and oxygen. Since X_{O} is ~ 3 eV and X_{Ta} is $\sim 1.2-1.6$ eV,¹⁰ the formation of a negative dipole leading to an increase in the work function would be expected. The data obviously violate this simple electronegativity model. A similar violation has also been observed in our recent study of nitrogen adsorption upon (110) Ta. Also, studies of oxygen adsorption upon (110), (100), and (111) nickel¹¹ and nitrogen adsorption upon (100) and (110) tungsten¹⁰ violate this principle.

A possible reason for this violation can be seen most clearly in the work of Farnsworth and Park¹² for oxygen adsorption upon (110), (100), and (111) nickel. On the basis of LEED, contact potential, and photoelectric measurements, they concluded that, with sufficient temperature activation, the work function decreased for lower coverage structures. Up to the formation of a certain high-coverage structure, the photoelectric data closely followed the Fowler plot for metals, thereby indicating that the oxygen-nickel binding was not extremely ionic. Also, once the high-coverage structure was

(XV. PHYSICAL ELECTRONICS AND SURFACE PHYSICS)

reached, and data failed to fit the Fowler plot, thereby indicating a change to a more ionic type of binding.

D. L. Fehrs, R. E. Stickney

References

1. D. L. Fehrs and R. E. Stickney, "Report on Twenty-Sixth Annual Conference on Physical Electronics, Massachusetts Institute of Technology, Cambridge, Mass., March 21-23, 1966," p. 287; D. L. Fehrs and R. E. Stickney, Quarterly Progress Report No. 82, Research Laboratory of Electronics, M.I.T., July 15, 1966, p. 77.
2. P. A. Anderson, *Phys. Rev.* 47, 958 (1935).
3. W. B. Nottingham, Thermionic Emission, Technical Report 321, Research Laboratory of Electronics, M.I.T., December 10, 1956.
4. S. Glasstone, K. J. Laidler, and H. Eyring, The Theory of Rate Processes, (McGraw-Hill Book Company, New York, 1961).
5. G. Ehrlich, *Ann. N.Y. Acad. Sci.* 101, 722 (1963).
6. B. J. Hopkins and K. R. Pender, *Surface Sci.* 5, 155 (1966).
7. Ya. P. Zingerman, V. A. Ishchuk, and T. A. Krutilina, *Soviet Phys. - Solid State* 7, 2078 (1966).
8. L. H. Germer and J. W. May, *Surface Sci.* 4, 452 (1966).
9. L. Pauling, The Nature of the Chemical Bond (Cornell University Press, Ithaca, N. Y., 3rd rev. ed., 1960).
10. T. A. Delchar and G. Ehrlich, *J. Chem. Phys.* 42, 2686 (1964).
11. H. E. Farnsworth, "Report on Twenty-Fifth Annual Conference on Physical Electronics, Massachusetts Institute of Technology, Cambridge, Mass., March 24-26, 1965," p. 140.
12. R. L. Park and H. E. Farnsworth, *J. Appl. Phys.* 35, 2220 (1964).

B. DESORPTION AND MIGRATION KINETICS OF MOLECULES ADSORBED ON NONUNIFORM SURFACES: STEADY-STATE ANALYSIS

1. Introduction

The rate of desorption of atoms and molecules from solid surfaces is a significant factor in a variety of engineering problems. For example, this rate often limits the performance of composite thermionic cathodes, the efficiency of catalytic processes, and the speed of surface oxidation. The practical importance of these applications has served to stimulate many experimental and theoretical investigations of desorption.¹⁻³

The majority of the existing analytical treatments of desorption are based on the assumption that the surface properties are uniform over the entire specimen. For polycrystalline specimens, however, it is known that this assumption leads to unsatisfactory results in detailed analyses of similar processes, such as thermionic emission⁴⁻⁶ and

(XV. PHYSICAL ELECTRONICS AND SURFACE PHYSICS)

surface ionization.^{6,7} The results of our recent experimental investigation of oxygen desorption from single-crystal tungsten⁸ have led us to attempt to develop a more exact desorption theory for patchy (for example, polycrystalline or nonuniform) surfaces. The first case that we have considered is that of steady-state desorption, and the analysis of a simple model is presented here. After refining this treatment, we plan to consider next the more general problem of flash (that is, transient) desorption.¹

2. Theoretical Model

To simplify this preliminary analysis we shall adopt a model that is based on a great number of assumptions, many of which may easily be refined or omitted in the final development. Here we shall concentrate on the inclusion of surface patches in the model.

Consider a two-patch model of a cylindrical wire having a circumference $2W$, where W is the width of each patch. The distance from the center of patch 1 around the wire is denoted by x . For a given atomic adsorbate, patches 1 and 2 have desorption energies V_1 and V_2 , migration energies E_1 and E_2 , adatom frequencies of vibration ν_1 and ν_2 , adsorbed atom densities n_1 and n_2 , and circumferential spacing between adsorption sites a_1 and a_2 . (See Fig. XV-5.) The boundary between the two patches is assumed

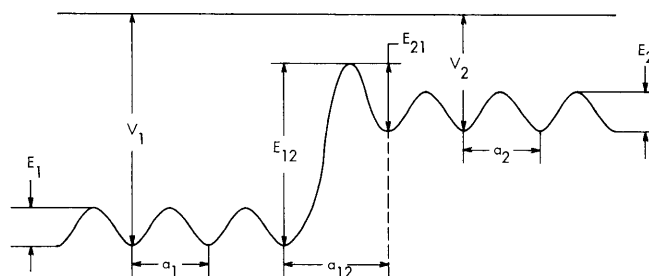


Fig. XV-5. Potential energy diagram for the two-patch model.

to have an energy barrier, with E_{12} and E_{21} being the barrier potentials for an atom migrating from patch 1 to patch 2 and vice versa. The distance between adsorption sites for an atom crossing the boundary is a_{12} . The probability that an atom with sufficient energy to migrate will actually do so is represented by A , where A is assumed to be only a function of surface geometry.

The linear particle flux across the boundary from patch 1 to 2, i_{12} , is given by

$$i_{12} = A_{12} n_1 \left(\frac{W}{2} \right) a_1 \nu_1 e^{-E_{12}/kT}, \quad (1)$$

where $e^{-E_{12}/kT}$ is the probability of an adatom having energy E_{12} or greater, and

$n_1\left(\frac{W}{2}\right) a_1$ is the linear atom density on patch 1 at the boundary. Likewise, the flux from patch 2 to 1 is

$$i_{21} = A_{21} n_2\left(\frac{W}{2}\right) a_2 v_2 e^{-E_{21}/kT}. \quad (2)$$

The net linear flux then is $i_{12} - i_{21}$.

If now the boundary is considered to lie in patch 1 and E_1 is the migration potential, the expression for the net flux across patch 1 at x is

$$i_1 = A_1 n_1(x) a_1 v_1 e^{-E_1/kT} - A_1 n_1(x+a_1) a_1 v_1 e^{-E_1/kT} \quad (3)$$

$$i_1 = -A_1 a_1^2 \frac{dn_1}{dx} v_1 e^{-E_1/kT}. \quad (4)$$

The desorbed flux j_1 is given by

$$j_1 = n_1(x) v_1 e^{-V_1/kT}, \quad (5)$$

where the probability of an adatom having sufficient energy to escape the surface is given by $e^{-V_1/kT}$, the number of particles per unit area is $n_1(x)$, and the number of attempts made per second is v_1 . From this equation we get

$$n_1(x) v_1 = j_1 e^{V_1/kT} \quad (6)$$

which may be substituted in $(i_{12} - i_{21})$ and i_1 :

$$i_{12} - i_{21} = e^{\frac{V_1 - E_{12}}{kT}} (a_1 A_{12} j_1 - a_2 A_{21} j_2) \quad (7)$$

$$i_1 = -A_1 a_1^2 e^{\frac{V_1 - E_1}{kT}} \frac{dj_1}{dx}. \quad (8)$$

Here the relation $V_1 - E_{12} = V_2 - E_{21}$ has been used (see Fig. XV-5). The steady-state continuity equation for a control area of width a_1 at point x on patch 1 is

$$i_1(x) + a_1 j_0 = i_1(x+a_1) + a_1 j_1, \quad (9)$$

where j_0 is the incident flux. This becomes

$$j_0 = j_1 + \frac{i_1(x+a) - i_1(x)}{a_1} = j_1 + \frac{di_1}{dx}. \quad (10)$$

(XV. PHYSICAL ELECTRONICS AND SURFACE PHYSICS)

Defining λ_1 and λ_2 as

$$\lambda_1^2 = a_1^2 A_1 e^{\frac{V_1 - E_1}{kT}} \quad (11)$$

$$\lambda_2^2 = a_2^2 A_2 e^{\frac{V_2 - E_2}{kT}} \quad (12)$$

and substituting the derivative of Eq. 4 in Eq. 10 yields

$$j_o = j_1 - \lambda_1^2 \frac{d^2 j_1}{dx^2} \quad (13)$$

$$j_o = j_2 - \lambda_2^2 \frac{d^2 j_2}{dx^2}. \quad (14)$$

Their solutions are

$$j_1 = j_o \left(1 + a_1 \cosh \frac{x - x_1}{\lambda_1} \right), \quad -\frac{W}{2} \leq x \leq \frac{W}{2} \quad (15)$$

$$j_2 = j_o \left(1 + a_2 \cosh \frac{x - x_2}{\lambda_2} \right), \quad \frac{W}{2} \leq x \leq \frac{3W}{2}. \quad (16)$$

Since patch 1 is symmetric about $x = 0$, and patch 2 is symmetric about $x = W$, the fluxes are

$$j_1 = j_o \left(1 + a_1 \cosh \frac{x}{\lambda_1} \right), \quad -\frac{W}{2} \leq x \leq \frac{W}{2} \quad (17)$$

$$j_2 = j_o \left(1 + a_2 \cosh \frac{x - W}{\lambda_2} \right), \quad \frac{W}{2} \leq x \leq \frac{3W}{2} \quad (18)$$

The constants a_1 and a_2 are determined by the boundary conditions

$$i_1 \left(\frac{W}{2} \right) = i_{12} - i_{21} = i_2 \left(\frac{W}{2} \right). \quad (19)$$

The resulting expressions for the fluxes are

$$\frac{j_1 - j_o}{j_o} = \frac{(A_{21} a_2 - A_{12} a_1) \cosh \frac{x}{\lambda_1}}{\lambda_1 \sinh \frac{W}{2\lambda_1} \left(\frac{A_{21} a_2}{\lambda_2 \tanh \frac{W}{2\lambda_2}} + \frac{A_{12} a_1}{\lambda_1 \tanh \frac{W}{2\lambda_1}} + e^{-\frac{(V_1 - E_{12})}{kT}} \right)} \quad (20)$$

$$\frac{j_2 - j_0}{j_0} = - \frac{(A_{21}a_2 - A_{12}a_1) \cosh \frac{x - W}{\lambda_2}}{\lambda_2 \sinh \frac{W}{2\lambda_2} \left(\frac{A_{21}a_2}{\lambda_2 \tanh \frac{W}{2\lambda_2}} + \frac{A_{12}a_1}{\lambda_1 \tanh \frac{W}{2\lambda_1}} + e^{-\frac{(V_1 - E_{12})}{kT}} \right)} \quad (21)$$

In the limit of small patches with $W \ll \lambda_{1,2}$ the fluxes are given by

$$\frac{j_1 - j_0}{j_1} = \frac{A_{21}a_2 - A_{12}a_1}{A_{21}a_2 + A_{12}a_1 + \frac{W}{2} e^{-\frac{(V_1 - E_{12})}{kT}}} \quad (22)$$

$$\frac{j_2 - j_0}{j_2} = - \frac{A_{21}a_2 - A_{12}a_1}{A_{21}a_2 + A_{12}a_1 + \frac{W}{2} e^{-\frac{(V_1 - E_{12})}{kT}}} \quad (23)$$

Thus we see that different fluxes from different planes are predicted. At present, we are considering the validity of applying the principle of detailed balance in problems of surface migration.

F. W. Eberle, R. E. Stickney

References

1. G. Ehrlich, "Modern Methods in Surface Kinetics: Flash Desorption, Field Emission Microscopy, and Ultrahigh Vacuum Techniques," Advances in Catalysis, Vol. 14, p. 255 (Academic Press, New York, 1963).
2. D. O. Hayward and B. M. W. Trapnell, Chemisorption (Butterworths Ltd., London, 2d edition, 1964).
3. G. C. Bond, Catalysis by Metals (Academic Press, New York, 1962).
4. W. B. Nottingham, "Thermionic Emission," Technical Report 321, Research Laboratory of Electronics, M.I.T., December 10, 1956.
5. C. Herring and M. H. Nichols, "Thermionic Emission," Rev. Mod. Phys. 21, 185 (1949).
6. L. N. Dobretsov, "Electron and Ion Emission," NASA Technical Translation, NASA TT F-73, 1952.
7. E. Ya. Zandberg and N. I. Ionov, "Surface Ionization," Soviet Phys. - Tech. Phys. 67, 255 (1959).
8. W. Engelmaier and R. E. Stickney, "Thermionic and Adsorption Characteristics of a Single-Crystal Tungsten Filament Exposed to Oxygen," Report on Twenty-sixth Annual Conference on Physical Electronics, Massachusetts Institute of Technology, Cambridge, Mass., March 21-23, 1966, p. 260.

(XV. PHYSICAL ELECTRONICS AND SURFACE PHYSICS)

C. SINGLE-PHONON ENERGY TRANSFER BETWEEN MOLECULAR BEAMS AND SOLID SURFACES

[This report summarizes a paper that will appear in The Physical Review.]

The quantum-mechanical lattice theory in thermal accommodation coefficient theory is approached from the same point of view as the lattice theory of neutron scattering and Mössbauer effects. Treating the surface atoms from a displacement field theoretic point of view, rather than from the customary single-particle point of view, is more consistent with other solid-state theories. Virtual phonon processes occurring in the field formulation give rise to a nontrivial modification in existing single-phonon accommodation coefficient theories. This modification takes the form of a pseudo Debye-Waller factor.

When the existing theoretical accommodation coefficients are modified by the pseudo Debye-Waller factor, it is found that the resulting accommodation coefficient, obtained herein, displays trends similar to experimental data for helium scattering off of tungsten.

J. W. Gadzuk

D. THEORY OF ATOM-METAL INTERACTIONS

[This report summarizes two papers that will appear in Surface Science.]

1. ALKALI ATOM ADSORPTION

The interaction of a metal with an alkali atom is considered from first principles. It is shown that treating the interaction of the metal with the alkali atom through perturbation theory is a meaningful approach. It is seen that the interaction causes a shift and broadening of the valence level of the alkali atom. Furthermore, it is seen that electron transitions between virtual atomic and metal states are formally equivalent to standard rearrangement processes.

The first-order ns energy-level shift of the alkalis is calculated and the results given in standard form. The shift is found to be $\sim +0.3$ eV. The natural broadening of the originally discrete ns level is calculated in closed form by using time-dependent perturbation theory. The theoretical bandwidth for an alkali atom adsorbed on a metal is found to be $\lesssim 1$ eV.

These results are discussed in relation to previously suggested values for the shifted and broadened level.

It is found that the position of the shifted and broadened level relative to the conduction band of the metal is such that ionic bonds are formed between adsorbate and substrate. The possibility and implications of localized electrons in the interior of the metal near the surface and also around the alkali ion cores are discussed. It is found

that electrons do tend to localize at the surface in the presence of alkali ion cores. The resulting surface dipoles are then discussed in relation to their effects on electron emission properties of the surface. Temperature dependences are included in a semi-quantitative manner, and the origin of thermal depolarization effects is displayed.

J. W. Gadzuk

2. ONE-ELECTRON TRANSITION MATRIX ELEMENTS

The matrix element describing a process in which an electron makes a transition from an atomic s state to a metal conduction band state is considered from the point of view of a rearrangement process. Since the initial and final states are not solutions of the same Hamiltonian, they are not orthogonal. It is shown that by orthogonalizing the initial and final stages, it is possible to obtain a simple, compact matrix element that describes electron transitions between the atom and metal states.

The matrix element is explicitly evaluated for a transition between a hydrogen-like atom and a free electron metal. These closed form results have been previously used to describe alkali-atom adsorption on metals. The present results could also be used to describe resonance ionization of atoms or neutralization of ions by metals.

J. W. Gadzuk

